Radiological characterisation of alkali-activated construction materials containing red mud, fly ash and ground granulated blast-furnace slag

Peer-reviewed author version

SAS, Zoltan; Sha, Wei; Soutsos, Marios; Doherty, Rory; Bondar, Dali; GIJBELS, Katrijn & SCHROEYERS, Wouter (2019) Radiological characterisation of alkali-activated construction materials containing red mud, fly ash and ground granulated blast-furnace slag. In: SCIENCE OF THE TOTAL ENVIRONMENT, 659, p. 1496-1504.

DOI: 10.1016/j.scitotenv.2019.01.006
Handle: http://hdl.handle.net/1942/28171

Radiological characterisation of alkali-activated construction materials containing red mud, fly ash and ground granulated blast-furnace slag

Zoltan Sas[1,2], Wei Sha[1,*], Marios Soutsos[1], Rory Doherty[1], Dali Bondar[1], Katrijn Gijbels[2], Wouter Schroeyers[2]

[1]*School of Natural and Built Environment, Queen's University Belfast, David Keir Bldg., 39-123 Stranmillis Road, Belfast BT9 5AG, United Kingdom*

[2] *Hasselt University, CMK, Nuclear Technological Centre (NuTeC), Faculty of Engineering Technology, Agoralaan, Gebouw H, 3590 Diepenbeek, Belgium*

**Corresponding author: w.sha@qub.ac.uk*

Abstract

Poor storage of industrial wastes has been a cause of land contamination issues. These wastes or by-products have the potential to be used as secondary raw materials in construction, promoting the concept of a circular economy that will avoid land contamination. Here we evaluate radiological environmental impacts when wastes that contain elevated levels of naturally occurring radionuclides (NORs) such as red mud, fly ash and ground granulated blast furnace slag are made into 'green cements' such as geopolymers or alkali-activated materials (AAMs). During the study, three AAM concrete and mortar series with various mixing ratios were prepared and investigated. The NOR content, I-Index, radon emanation and exhalation of the precursor waste materials and their cement products were

measured and calculated and the strength of the cement products was compared. The emanation and the exhalation properties were calculated for the final products, weighing the data of the components as a function of their mixing ratio. The I-index alone suggested that the AAMs would be suitable products. AAMs containing ground granulated blast furnace slag exhibited the lowest radon exhalation and higher compressive strength, while the fly ash and red mud AAMs had increased final radon exhalation. In the case of fly ash, alkaline activation of fly ash dramatically increased the radon exhalation; the highest measured fly ash exhalation was 1.49 times of the theoretically calculated exhalation value. This highlights the increased risk of using fly ash as a component in AAMs and the need to carry out testing on the final products as well as individual secondary raw materials.

Keywords: Gamma spectrometry; Radon emanation; Radon exhalation; Geopolymer; Alkali-activated material; Secondary raw materials

Highlights

- Three alkali-activated materials were prepared using secondary raw materials
- The radiological properties of the secondary raw materials and AAMs were determined
- The fly ash content increased the radon exhalation during alkali activation
- Increasing GGBFS content resulted in better radiological and strength property

1. Introduction

Increasing use of recovered wastes or secondary raw materials in construction products is a crucial step to tackle the depletion of primary raw materials and promote the development of a circular economy (European Commission, 2015). However, before industrial secondary raw materials can be allowed for reuse or recycling in the built environment, it is crucial to assess and control any impact on human health or the environment. Indoor air quality is affected by numerous factors, e.g. chemicals, radon, particulate matter, dust and moulds that can have an adverse effect on the health of the inhabitants (EEA-JRC, 2013). To avoid a potential negative impact on the indoor air quality, advanced but straightforward techno-economical solutions are required. These include science-based policies of monitoring and control of construction materials during production, throughout the construction lifespan and eventually in future reuse. Secondary raw materials have the potential to be utilised in large quantities, e.g. as solid binders in alkali-activated material (AAM) type cements with performance comparable to Portland cement. For the production of new 'green' forms of concrete (Bontempi, 2017), the use of AAMs incorporating industrial secondary raw materials can significantly reduce the CO_2 emissions (Van Deventer et al., 2010).

A specific problem with the use of industrial secondary raw materials is that they may contain elevated concentrations of naturally occurring radionuclides or NORs (Kovacs et al., 2017a; Sas et al., 2017; Schroeyers et al., 2018), which can significantly contribute to the radiation dose of residents (United Nations Scientific Committee on the Effects of Atomic Radiation, 2010). This occurs via two exposure pathways. The first is external exposure directly caused by the emitted gamma radiation from the NOR present in the building materials. Some recent papers presented the latest collections of activity concentration data of natural radionuclides (Ra-226, Th-232 and K-40) in building materials (Sas et al., 2017; Schroeyers et al., 2018; Trevisi et al., 2018). These collections also include radiological information about some NORM residues and by-products (by-product gypsum, metallurgical slags, fly and bottom ashes and red mud) which can be of radiological concern if reused in building materials as secondary raw materials. The second pathway is the internal exposure by the inhalation of radon (Rn-222) and its radioactive short and long-lived progenies which can be found in the decay series of U-238. After inhalation of radon, the radon progenies (mainly alpha and beta emitters) are predominantly responsible

for the irradiation of the cells of the pulmonary system. Radon is estimated to cause between 3 and 14% of all lung cancers, depending on the average background radon levels. In Europe, this corresponds to 20,000 deaths every year (Darby et al., 2005; Dubois and Bossew, 2006).

The exposure of inhabitants from building materials that contain NORs comes mainly from radon. According to the EU-BSS, the reference level for indoor radon is 300 Bq/m^3 which should be kept in both dwellings and workplaces (European Union, 2014). WHO (2016) recommends only 100 Bq/m^3 average radon concentration. Natural soils constitute the main source of the indoor radon, but the contribution from building materials is becoming more significant as the use of 'green cement' increases. Radon levels in buildings can vary greatly over time (Sainz et al., 2009). Due to the increase of energy efficient building designs, reduction in ventilation rates increases the indoor radon levels (Vasilyev et al., 2017). The radon exhalation of building materials dramatically depends on the properties of the material matrix such as the Ra-226 activity concentration, its distribution within the matrix, the moisture content, thickness of the material, the permeability which influences the radon diffusion length (Keller et al., 2001), and the emanation factor (Sahoo et al., 2011). The emanation factor is the ratio between the amount of the radon atoms exiting the matrix into the pore space and the total amount of radon atoms generated in the matrix. These parameters determine the final exhalation properties of the material matrixes. It is not possible to remove the Ra-226 content from building materials, so the screening of secondary raw materials in advance can help to avoid elevated levels of Ra-226 as a radon source. Good design, especially the reduction of the emanation factor, is the key to reducing the exhalation rate of construction materials (Hegedus et al., 2016; Kovacs et al., 2017b; Sas et al., 2013, 2015a). The formation of final matrix properties can affect the emanation and the exhalation properties depending on the components, their mixing proportions, the Ra-226 content and their interaction (Gijbels et al., 2018). A tool that considers radon can be useful for controlling the exposure of inhabitants especially for the recycling of industrial secondary raw materials in AAMs where additional measurements are desirable. However, there is no standardised, industrially useful method for screening the radon and its release rate from building materials. In general, radon exhalation should be kept as low as possible in construction materials. There is a lack of information regarding the impact of construction materials on the emission of radon, especially from new green cements such as alkali-activated materials.

The aim of this research is to determine the NOR content of the industrial secondary raw materials (red mud, fly ash and ground granulated blast furnace slag) alongside sand, aggregate, and the final alkali-activated materials using gamma spectrometry. In addition, we aim to measure the massic exhalation and the radon emanation factor using the closed accumulation chamber technique, so that we are able to compare the emanation and exhalation properties of the secondary raw materials and the final alkali-activated materials considering mixing ratios together with the components' emanation and exhalation data. The geopolymerisation process may result in a geopolymerisation product that have rather different exhalation and emanation properties than the sum of its raw materials. The purpose of the radiological characterisation in this research is to provide a clear and conclusive test of this research hypothesis. The second research hypothesis is that there is a link between the strength and the radiological characteristics of geopolymers. Measuring the 28 days compressive strength property of the final alkali-activated materials is aimed at testing this second research hypothesis.

2. Materials and methods

2.1 Raw materials

Three different types of industrial secondary raw materials – fly ash (FA), ground granulated blast furnace slag (GGBFS) and red mud (RM), alongside sand (SAND) and basalt aggregate (AGG) were used to prepare AAM concrete and mortar sample series. The FA is generated during coal combustion. The amount of the generated residue depends on the inert mineral content, which can vary between 5 and 30%. This residue consists of the non-combustible inorganic part of the coal that remains after the burning as ash or a slag type residue. The GGBFS is produced during iron production. The production of iron from raw materials (iron ore, pellets, sinter, flux and slag producing material such as limestone or dolomite, coke for fuel) uses blast furnaces. Blast furnace slag is also generated which is then granulated and ground into a by-product (Kovacs et al., 2017a). The fly ash used in this study was siliceous and was obtained from Power Minerals Ltd., Drax Power Station, North Yorkshire, UK. The slag was supplied by Civil and Marine Ltd-Hanson Company, member of the Heidelberg Cement Group, Essex, UK. The fly ash and slag conform to BS EN 450-1 (2012) and BS EN 15167-1 (2006), respectively. Red mud is a slurry type alkaline material, the by-product of aluminium production, which is generated as a result of the Bayer

process using hot (150-200°C) NaOH solution to digest the ore (Kovacs et al., 2017a). It has a dark red colour owing to its high iron content. The disposal of the red mud is problematic owing to its properties, e.g. high alkalinity (pH ≥11), high water content ~60%, and its physical features similar to wet clay (Ayres et al., 2001) which has caused land contamination issues. Red mud was received from Aughinish Alumina Ltd., Limerick, Ireland. The chemical composition of the component materials was determined by the X-ray fluorescence (XRF) method (Fig. 1). The equipment used was a PANalytical Axios Advanced XRF spectrometer. XRF analysis was carried out on fused glass beads prepared from ignited powders of the materials. The results, which were quoted as weight percent, were analysed using PANalytical SuperQ software using reference samples and artificial analogues. LOI was determined by igniting the materials at 950°C for 1.5 h.

Composition of major elements in Oxide form (%)

0.0 — 100.0

Sample ID	SiO2	TiO2	Al2O3	Fe2O3	MnO	MgO	CaO	K2O	Na2O	P2O5	SO3	V2O5	Cr2O3	SrO	ZrO2	BaO	NiO	CuO	ZnO	PbO	LOI
AGG	44.81	2.09	17.10	15.29	0.22	7.34	8.39	0.17	2.63	0.17	0.00	0.05	0.00	0.03	0.02	0.05	0.01	0.01	0.01	0.00	2.70
FA	50.24	0.98	25.84	11.27	0.08	1.86	3.15	2.91	0.89	0.22	0.12	0.08	0.02	0.10	0.03	0.32	0.02	0.02	0.03	0.01	3.05
GGBFS	34.74	0.62	13.80	0.34	0.46	7.63	41.13	0.69	0.30	0.00	2.54	0.01	0.00	0.08	0.04	0.42	0.00	0.00	0.00	0.00	0.00
RM	8.58	10.17	16.25	43.76	0.05	0.07	5.64	0.09	4.68	0.32	0.16	0.23	0.25	0.01	0.35	0.21	0.00	0.00	0.00	0.01	9.33
SAND	71.14	0.80	11.75	5.68	0.08	1.92	2.18	2.04	1.93	0.09	0.00	0.02	0.01	0.02	0.03	0.11	0.00	0.00	0.01	0.00	1.84

Sample ID	As	Ba	Ce	Co	Cr	Cs	Cu	Ga	La	Mo	Nb	Nd	Ni	Pb	Rb	Sb	Sc	Se	Sn	Sr	Th	U	V	W	Y	Zn	Zr
AGG	0	91	20	50	25	0	129	19	3	2	4	14	72	52	4	5	20	0	23	326	2	1	185	0	35	270	146
FA	148	1220	132	45	145	10	180	57	74	29	22	59	163	156	140	15	33	17	5	882	22	10	449	3	65	283	227
GGBFS	1	1611	126	0	11	0	1	0	71	2	7	56	0	0	17	0	0	0	0	680	14	9	34	0	73	9	294
RM	71	19	125	8	1142	7	60	99	63	10	180	35	0	71	6	4	52	4	29	124	129	15	926	16	112	63	2729
SAND	3	600	46	21	119	0	29	16	23	2	13	23	41	14	72	0	19	0	0	183	8	2	134	0	22	73	234

Composition of trace elements (ppm)

0 — 3000

Fig. 1. Major and trace element composition of secondary raw materials (FA = fly ash, GGBFS = ground granulated blast furnace slag, RM = red mud), aggregates (AGG) and sand (SAND).

2.2 Alkali-activated material casting and curing

All the components for the emanation and exhalation study were dried to constant mass at 105°C for 24 h. For the emanation and exhalation study, it is necessary to remove the entire moisture content from the matrix because it

can dramatically increase the emanation factor. Only 1-2% moisture content can increase it by 50-100%. This temperature is commonly used before radon exhalation measurements. The main focus of the research was to investigate the radiological properties of AAM containing secondary raw materials with a variety of mixing ratios. For this investigation, GGBFS containing concrete mixes, i.e. G series (Bondar et al., 2016) and FA and GGBFS containing mortar mixes, i.e. F/G series with a constant sand to binder ratio (Rafeet, 2016) were used. Red mud and GGBFS mixes (R/G series) were also prepared using the same constant sand to binder ratio as the F/G series. As such, the mix design has followed previous experience in the research group, but it should be noted that there is no standard mix design method for AAM concrete and therefore the mix designs used in this work were essentially through trial and error, completed in previous experiments as cited above. All components were separately dried to constant mass at 105°C for 24 h. Next, the materials were separately added to the mixer, firstly the sand (sand and aggregate in the case of G series), secondly the binder material. The mixes were dry blended for 2 min until a homogeneous mixture was acquired. Sodium hydroxide solution, sodium silicate solution (in the case of G and F/G series) and water were combined and then added to the mixture and stirred continuously for 5 min. For F/G series, the upper limit was 70% (w/w) to the GGBFS content because a mix with higher weight ratio had a setting time of about 5 min, which is too short to be manageable for construction purposes. This procedure was also used by Rafeet (2016) to examine a variety of mechanical properties of these similar mixes. In the case of the red mud secondary raw material, the alkalinity of the red mud was sufficient without the need for any alkali activating solution. The mixing proportions of the sample series are listed in Table 1. In this table, water (kg/m^3) includes the water in the alkali solutions, to make the water to binder ratio parameter comparable with water to cement ratio in Portland cement mixes. For this reason, actual kg/m^3 values of the alkali solutions are not given in the table, to avoid double counting the amounts of water in these solutions. Also, as the alkali solutions from different sources can have different concentrations, the kg/m^3 of the alkali solutions needed will vary, even for the same NaOH % and M_S values, if the solution concentrations change. Providing NaOH % and M_S values only will accommodate whatever concentrations of these solutions used in practice. In the table, NaOH in wt% of the total FA and GGBFS amount is given. M_S is the SiO_2/Na_2O ratio in alkali solutions.

Table 1. Mixing proportions of component including fly ash (FA), red mud (RM), ground granulated blast furnace slag (GGBFS), sand (SAND) and aggregates (AGG) used for alkali-activated material (AAM) sample casting of the ground granulated blast furnace slag (G), fly ash and ground granulated blast furnace slag (F/G) and red mud and ground granulated blast furnace slag (R/G) series.

Mix	FA or RM (kg/m^3)	GGBFS (kg/m^3)	SAND (kg/m^3)	AGG (kg/m^3)	Water (kg/m^3)	Water to binder ratio	NaOH (wt%)	M_S
G 1	-	300	778	1158	180	0.60	4	0.45
G 2	-	360	677	1008	250	0.70	4	0.45
G 3	-	400	675	1005	240	0.60	4	0.45
G 4	-	400	697	1037	220	0.55	4	0.45
G 5	-	400	675	1005	240	0.60	6	0.45
G 6	-	400	697	1037	220	0.55	6	0.45
G 7	-	400	697	1037	220	0.55	8	0.45
G 8	-	400	697	1037	220	0.55	4	1.00
F/G 70/30	350	150	1375	-	185	0.37	5.8	0.80
F/G 60/40	300	200	1375	-	185	0.37	5.8	0.80
F/G 50/50	250	250	1375	-	185	0.37	5.8	0.80
F/G 40/60	200	300	1375	-	185	0.37	5.8	0.80
F/G 30/70	150	350	1375	-	185	0.37	5.8	0.80
R/G 50/50	250	250	1375	-	185	0.37	-	-
R/G 40/60	200	300	1375	-	185	0.37	-	-
R/G 30/70	150	350	1375	-	185	0.37	-	-
R/G 20/80	100	400	1375	-	185	0.37	-	-
R/G 10/90	50	450	1375	-	185	0.37	-	-

The mixed specimens were put into the moulds and compacted on a vibrating table. For the G series, ϕ100×200 mm cylinders and 100×100×100 mm cubes were used. For the F/G and R/G series, 50×50×50 mm cubes were used. Such small cubes for mortar mixes were used successfully in recent work by the group, in, e.g., Aiken et al. (2018). The samples of G series were made in previous experimental work and were used here to study the radiological properties. The samples of F/G and R/G series were prepared in this work. Concrete samples, as in the case of G series, needed to have larger sizes than mortar samples, as in the case of F/G and R/G series. Form the radiological point of view, the sample dimensions do not have an effect on the NOR content and the massic exhalation. The moulded specimens were covered with plastic sheets and left in the casting room for 24 h at room temperature except for the R/G series. As a result of a trial experiment, it was found that curing at room temperature of R/G series did not cause any hardening. Therefore, the R/G mixes were cured at 70°C at first for 24 h. After 24 h of curing each sample series, they were demoulded and kept in a sealed plastic zip bag to avoid drying. The zip bags of the G and the F/G series were stored at room temperature, while the bags of the R/G series were stored at 70°C until testing.

2.3 The compressive strength of alkali-activated materials

The compressive strength was tested using a 3000 kN Matest compression testing machine motorised with a Servo-Plus Evolution control unit for fully automatic tests, to test cubes up to 200 mm side and cylinders up to ϕ160×320 mm. For the F/G and the R/G cubic mortar series, the compression rate was set at 0.6 MPa/s and the start load was set at 0.5 kN. The compressive strength tests were performed according to BS 12390-3 (2009).

2.4 Determination of naturally occurring radionuclide with gamma spectrometry

For gamma spectrometry, the dried, ground and sieved components (<5 mm) and AAM samples after 28 days curing were stored in radon-proof polystyrene sample holders equipped with a dense threaded stainless-steel cap for 27 days to achieve the secular equilibrium between the Ra-226 and the Rn-222 and its short-lived decay products of Pb-214 and Bi-214. The gamma spectrometry was performed with a high purity broad energy germanium detector (Canberra BE5025-7500SL) with a 50% nominal relative efficiency shielded with copper-

lined lead shield designed for low-activity measurements. Canberra ISOCS/LabSOCS was used for efficiency calibration by inserting all relevant parameters, including sample composition and density, geometry dimensions, materials and detector configuration and position, for each measurement. Sample measurement time was 80,000 s and spectra were corrected by subtracting the background spectrum. To obtain the Th-232 content, the gamma line of Pb-212 at 238 keV and Tl-208 at 583 keV were used. The Ra-226 activity concentration was determined via the Rn-222 progenies (Pb-214 at 351 keV and Bi-214 at 609 keV) while the K-40 content was calculated from the data of 1461 keV gamma peak (Shakhashiro et al., 2012).

2.5 Massic radon exhalation rate

The accumulation chamber technique is commonly used to determine the massic exhalation rate (Friedmann et al., 2017). After the gamma spectrometry, the samples were enclosed in radon-tight polycarbonate accumulation chambers equipped with stainless steel valves. A polycarbonate cap was tightened and fitted with an O-ring gasket to the columns. To ensure the radon free initial sample conditions at the beginning of the accumulation period, the chambers were vacuumed three times and finally aerated with radon free airflow (Sas et al., 2015b). During sampling, the accumulation chamber was connected to a looped leakproof radon pump with 5 L/min flow rate and an RD200 (200 cm^3 chamber with a counting efficiency of 0.81 CPH/Bq/m^3) ionisation chamber manufactured by FTLab placed in acrylic housing. The detector has ±10% measurement precision at 370 Bq/m^3. To ensure the secular equilibrium between the Rn-222 and its short half-life alpha emitting progenies of Po-218 and Po-214 and to avoid the Rn-220 contribution, the results of the first 3 h from the sampling were ignored (Jonas et al., 2016). The massic exhalation was calculated according to the following formula (Sas et al., 2015a):

$$E_{Mass} = \frac{C_t \cdot V}{m \cdot t} \cdot \frac{\lambda \cdot t}{1 - e^{-\lambda t}}$$

where C_t = accumulated radon concentration in the measurement kit during sampling [Bq/m^3], E_{Mass} = massic exhalation rate [mBq/(kg h)], t = accumulation time [h], V = volume of the accumulation kit [m^3], m = mass of the sample [kg], λ = leakage corrected decay constant of radon [h^{-1}].

2.6 Calculation of emanation factor

The emanation factor of the samples was calculated from the Ra-226 content obtained with gamma spectrometry and the equilibrium radon concentration calculated from the massic exhalation of the samples:

$$\varepsilon = \frac{Rn_{eq}}{C_{Ra-226}} \cdot 100$$

where ε = emanation factor (%), Rn_{eq} = equilibrium radon concentration and $C_{Ra\text{-}226}$ = Ra-226 activity concentration.

2.7 Error calculations

For compressive strength testing, three cube samples were tested for each condition. Average values are reported in Section 3.1. In the case of F/G and R/G series, standard deviation is reported. In the case of G series, blanket errors of 3 or 5 MPa are used, taken from Bondar et al. (2016) where the strength data was first reported.

In the determination of naturally occurring radionuclide with gamma spectrometry, the 1 sigma error was calculated by the LabSOCS sofware and reported in Section 3.2.

For massic radon exhalation, error values were derived from the sensitivity of the instrument, using information provided by manufacturer, and reported in Seciton 3.3. The errors of the exhalation results were used to calculate the errors of emanation; the two parameters have the same relative error.

For the linear regression reported in Section 3.3, the trendlines were placed with 95% confidence bands to represent the uncertainty in an estimate of a curve or function based on limited or noisy data. As confidence intervals refer to a single point, they are narrower (at this point) than a confidence band which considers many points (Härdle et al., 2004).

3. Results and discussion

3.1 Compressive strength of alkali-activated materials

The compressive strength of the AAM sample series is presented in Table 2. Data for G series is from Bondar et al. (2016). Data for F/G series is from Rafeet (2016).

Table 2. Compressive strength of samples at 1 day, 2 days, 7 days and 28 days in megapascals (MPa) giving averages of three replicates and blanket errors in ground granulated blast furnace slag (G) series and standard deviations in fly ash and ground granulated blast furnace slag (F/G) and red mud and ground granulated blast furnace slag (R/G) series.

Mix	1 day	2 days	7 days	28 days
G 1	-	15±3	19±5	27±5
G 2	-	11±3	14±5	22±5
G 3	-	15±3	20±5	26±5
G 4	-	18±3	22±5	30±5
G 5	-	21±3	26±5	36±5
G 6	-	25±3	32±5	44±5
G 7	-	38±3	47±5	54±5
G 8	-	26±3	34±5	48±5
F/G 70/30	9.9±1.5	-	18.1±0.6	47.9±2.7
F/G 60/40	17.6±3.2	-	44.7±3.7	47.9±5.6
F/G 50/50	15.6±1.0	-	38.2±2.4	50.3±0.2
F/G 40/60	26.1±1.3	-	45.8±3.4	63.0±0.7
F/G 30/70	24.7±2.3	-	71.6±11.5	77.0±7.0
R/G 50/50	0	0	4.0±0.4	6.5±0.3
R/G 40/60	0	4.3±0.3	3.9±0.9	6.4±0.3
R/G 30/70	0	6.5±0.1	5.8±0.4	7.0±0.5
R/G 20/80	0	6.9±0.4	6.5±0.9	7.1±0.2
R/G 10/90	0	7.1±0.4	6.4±0.5	8.0±0.1

Different sample series had different type of AAMs. Some were concrete, and some were mortar, with different sample sizes. So, results from different series cannot be compared. In the case of the G series of AAM concrete,

the highest compressive strength of 54 MPa after 28 days was found for the G7 mix. The F/G and the R/G mortar sample series were prepared with a constant sand/binder ratio. The FA containing sample series showed the increasing compressive strength tendency with the decreasing FA content. The R/G series was made without activators due to the high pH of red mud. However, the compressive strength results of that series were meagre compared to other mixes.

3.2 Naturally occurring radionuclide content

The activity concentration values of NORs obtained with gamma spectrometry are presented in Table 3. The Ra-226, the Th-232 and the K-40 content of the components range between 0.6 and 186 Bq/kg, 1.0 and 452 Bq/kg, and 34 and 743 Bq/kg with an average of 93 Bq/kg, 120 Bq/kg, and 282 Bq/kg, respectively. The basalt aggregate and the sand samples had the lowest NOR content resulting in I-index values of 0.02 and 0.32, respectively. In the case of the secondary raw materials, the red mud had the highest Ra-226 (186 Bq/kg) and Th-232 (452 Bq/kg) activity concentration values. The K-40 content was the highest in the case of the FA sample (743 Bq/kg).

Table 3. Naturally occurring radionuclide (NOR) content and radon exhalation and the emanation properties of secondary raw materials (FA = fly ash, GGBFS = ground granulated blast furnace slag, RM = red mud), aggregates (AGG) and sand (SAND) where the 1 sigma error for NOR contents was calculated by the LabSOCS software and the errors for exhalation and emanation were derived from the sensitivity of the instrument.

Material	Ra-226 (Bq/kg)	Th-232 (Bq/kg)	K-40 (Bq/kg)	Exhalation (mBq/kg h)	Emanation (%)
FA	139±10	82±6	743±31 (max.)	13±2	1.2±0.1
GGBFS	126±9	44±3	117±6	6±1	0.6±0.1 (min.)
RM	186±13 (max.)	452±31 (max.)	37±2	121±8 (max.)	9±1
AGG	0.6±0.2 (min.)	1.0±0.2 (min.)	34±2 (min.)	0.7±0.2 (min.)	15±5 (max.)
SAND	13±1	22±2	477±20	7±1	7±1
Average	93	120	282	30	7

The NOR content of the secondary raw materials was compared with recently published NOR databases, including By-BM NOR Database (Sas et al., 2017, 2019), NORM4Building database (Schroeyers et al., 2018; Sas et al. 2019), and EU NOR Database (Table 4) (Trevisi et al., 2018).

Table 4. Naturally occurring radionuclide (NOR) content (Bq/kg) of secondary raw materials (FA = fly ash, GGBFS = ground granulated blast furnace slag, RM = red mud) in Becquerel/kilogram found in the updated European NOR database.

Material	Ra-226			Th-232			K-40		
	Min	Max	Average	Min	Max	Average	Min	Max	Average
FA	75	815	191	37	140	91	157	900	561
GGBFS	15	336	139	1	152	65	20	786	249
RM	97	301	205	118	539	327	50	215	95

The Ra-226 content of all the secondary raw materials was lower than the average value in the NOR databases. The Th-232 activity concentration was found to be lower than the average value in the case of the FA and the GGBFS in all the databases. The measured Th-232 content for red mud was higher than the average reported in the By-BM and the EU NOR databases. The K-40 content of the FA was higher than all the database values while the GGBFS and the red mud contained lower K-40 activity concentration than the average values in all datasets. Overall, despite certain excess isotope activity concentrations, all results approximate well with the average values reported in the NOR databases. The NOR content of the prepared samples series is given in Table 5. All the samples in each series had I-index value significantly lower than 1.0. The highest result was obtained in the case of the red mud-containing AAMs.

Table 5. Naturally occurring radionuclide (NOR) content, calculated I-index and radon exhalation and the emanation properties of the three studied different alkali-activated material (AAM) sample series where the 1 sigma error for NOR contents was calculated by the LabSOCS software and the errors for exhalation and emanation were derived from the sensitivity of the instrument.

Mix	Ra-226 (Bq/kg)	Th-232 (Bq/kg)	K-40 (Bq/kg)	I-index	Exhalation (mBq/kg h)	Emanation (%)
G 1	21±2 (min.)	14±1 (min.)	179±8	0.20 (min.)	9.1±1.3 (max.)	6.0±0.9 (max.)
G 2	25±2	16±1	194±9	0.22	5.5±1.0	3.1±0.6
G 3	25±2	15±1	176±8	0.22	6.6±1.0	3.5±0.5
G 4	25±2	14±1 (min.)	154±8	0.20 (min.)	3.7±0.7	1.9±0.4
G 5	28±2	16±1	156±8	0.23	7.3±1.1	3.9±0.6
G 6	28±2	16±1	181±8 (max.)	0.23	2.6±0.7	1.4±0.4
G 7	29±2 (max.)	17±1 (max.)	170±8	0.24 (max.)	2.5±0.5 (min.)	1.3±0.3 (min.)
G 8	25±2	15±1	141±7 (min.)	0.20 (min.)	8.4±0.9	4.5±0.5
Average	26	16	160	0.22	5.7	3.2
F/G 70/30	38±3 (min.)	31±2 (min.)	511±22	0.45	10.4±1.4 (max.)	3.4±0.5 (max.)
F/G 60/40	42±3	34±2	548±23 (max.)	0.49 (max.)	6.8±0.9	2.2±0.3
F/G 50/50	44±3 (max.)	36±3 (max.)	502±21	0.49 (max.)	5.2±0.8	1.7±0.3
F/G 40/60	43±3	36±3 (max.)	488±21	0.48	4.3±0.6	1.4±0.2
F/G 30/70	39±3	34±2	400±19 (min.)	0.44 (min.)	3.4±0.6 (min.)	1.1±0.2 (min.)
Average	41	34	490	0.47	6.0	2.0
R/G 50/50	48±3 (max.)	78±5 (max.)	288±13 (min.)	0.65 (max.)	15.9±2.0 (max.)	4.6±0.6 (max.)
R/G 40/60	45±3	62±4	343±15	0.57	13.5±1.8	4.0±0.5
R/G 30/70	43±3	56±4	339±15	0.54	11.8±1.4	3.6±0.4
R/G 20/80	46±3	50±3	359±2 (max.)	0.52	10.4±1.2	3.3±0.4
R/G 10/90	42±3 (min.)	37±3 (min.)	351±15	0.44 (min.)	9.0±0.7 (min.)	2.9±0.2 (min.)
Average	45	57	336	0.54	12.1	3.7

3.3 Radon emanation and massic exhalation

The radon exhalation and the emanation properties of the component materials and of the AAM series are included in Tables 3 and 5, respectively. As was expected from the results of the secondary raw materials, the red mud-containing mixes had, on average, the highest exhalation and emanation. The FA containing mixes demonstrated the second highest exhalation rates, but surprisingly their average emanation factor was the lowest among the three studied AAM mix series.

The effect of microstructural changes that occur during the formation of AAMs can have a significant effect on the emanation and exhalation properties (Sas et al., 2015a) of the final product. To investigate the effect of the AAM formation on these parameters, the measured emanation factors and massic exhalation values of the samples were compared to theoretically calculated reference levels which were obtained by the weighting of the emanation and exhalation properties of the components as a function of sample mixing proportions. The reference levels for the emanation factors and the massic exhalations were calculated with the following equations:

$$\bar{\varepsilon} = \frac{\sum_{i=1}^{n} \varepsilon_i m_i}{\sum_{i=1}^{n} m_i}$$

where $\bar{\varepsilon}$ is the calculated weighted emanation factor (reference value of the mixture), ε_i is the emanation factor of the certain component used in the mixture, m_i is the mass of the component in the mixture.

$$\overline{E_{mass}} = \frac{\sum_{i=1}^{n} E_{mass_i} m_i}{\sum_{i=1}^{n} m_i}$$

where $\overline{E_{mass}}$ is the calculated weighted emanation factor (reference value of the mixture), E_{mass_i} is the massic exhalation of the certain component used in the mixture, m_i is the mass of the component in the mixture. This method is not suitable directly for prediction of the final emanation and exhalation properties of mixes, because these parameters greatly depend on the nanostructure of the formed matrix. However, it does provide a reasonable

check of the relative changes and identifies the effect of different mixing ratios on radon emanation and exhalation properties. In Fig. 2, the measured and calculated emanation and exhalation values are illustrated.

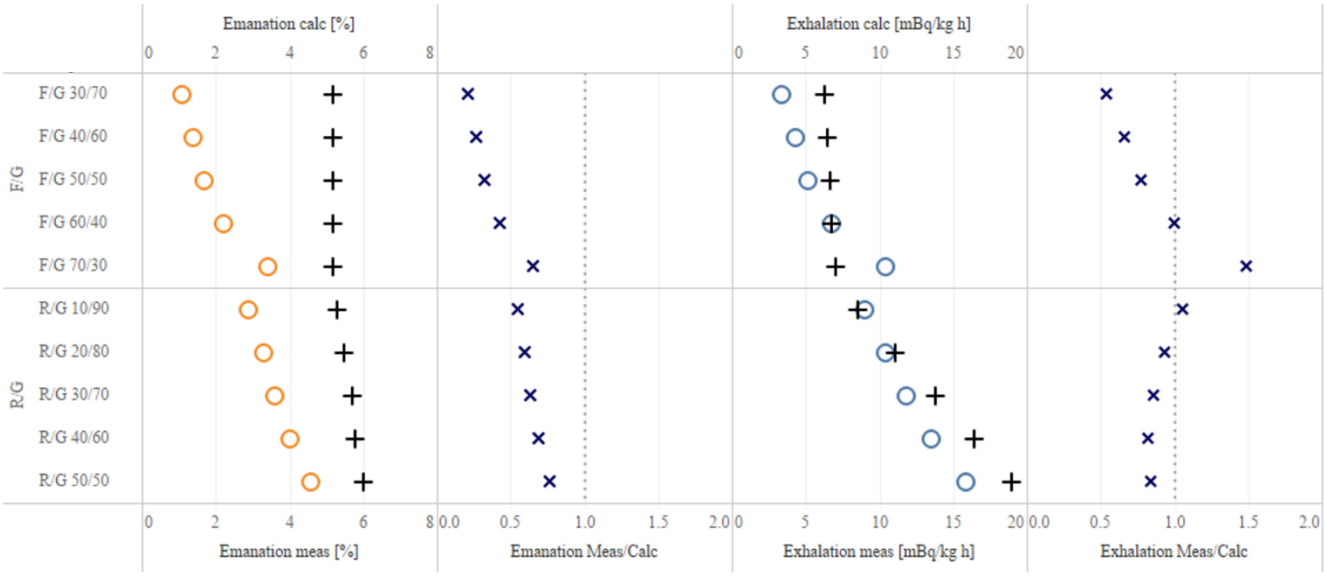

Fig. 2. The measured (marked with circles) and calculated (marked with +) emanation and exhalation values and their ratios (marked with ×) in the case of fly ash and ground granulated blast furnace slag (F/G) and red mud and ground granulated blast furnace slag (R/G) series.

With each series of AAM mixes, there was an increasing trend observed for both the measured and the calculated emanation and exhalation values that related to the increasing fly ash or red mud content.

Although all the measured and the calculated observations showed an increasing trend, the comparison of the value pairs (measured and calculated values of individual mixes) showed that the formation of the AAM matrixes influenced the emanation and exhalation properties more than would be expected if only the initial properties of the components are considered. The Measured/Calculated emanation values were significantly below 1.

The final exhalation property showed different behaviour in the fly ash and the red mud-containing AAMs (Fig. 2). In the case of fly ash AAM (F/G series), the lowest FA containing mix had a 0.54 ratio, while for the highest FA content the final exhalation was 1.49 times of the theoretically calculated exhalation value. We have demonstrated that as fly ash content increases there is also a substantial increase in the final exhalation values.

This is not expected at all. In general, fly ash has closed spherical structure which does not open significantly in the case of normal concretes. The alkali activation has very different effect on the fly ash resulting in intensified exhalation. The Measured/Calculated exhalation ratio of the red mud-containing R/G series showed the opposite tendency. The increasing red mud content decreased the Measured/Calculated exhalation ratio from 1.06 to 0.82. From these results, it can be concluded that the fly ash containing AAMs can pose an elevated risk due to radon exhalation. This emphasises the necessity of measuring radon exhalation characteristics as a function of the fly ash content and other influencing parameters, e.g. water content, activating solution to monitor the exhalation properties of the final product. In the case of the G series, neither the component ratios nor the activating solution were kept constant, which resulted in scattered output, from which it was not possible to make conclusions from the exhalation values.

To investigate the role of individual components on the final emanation and exhalation properties of the series directly, the measured emanation and exhalation parameters were compared with the FA, GGBFS and red mud, GGBFS content in the F/G and R/G series, respectively. The results are presented in Fig. 3.

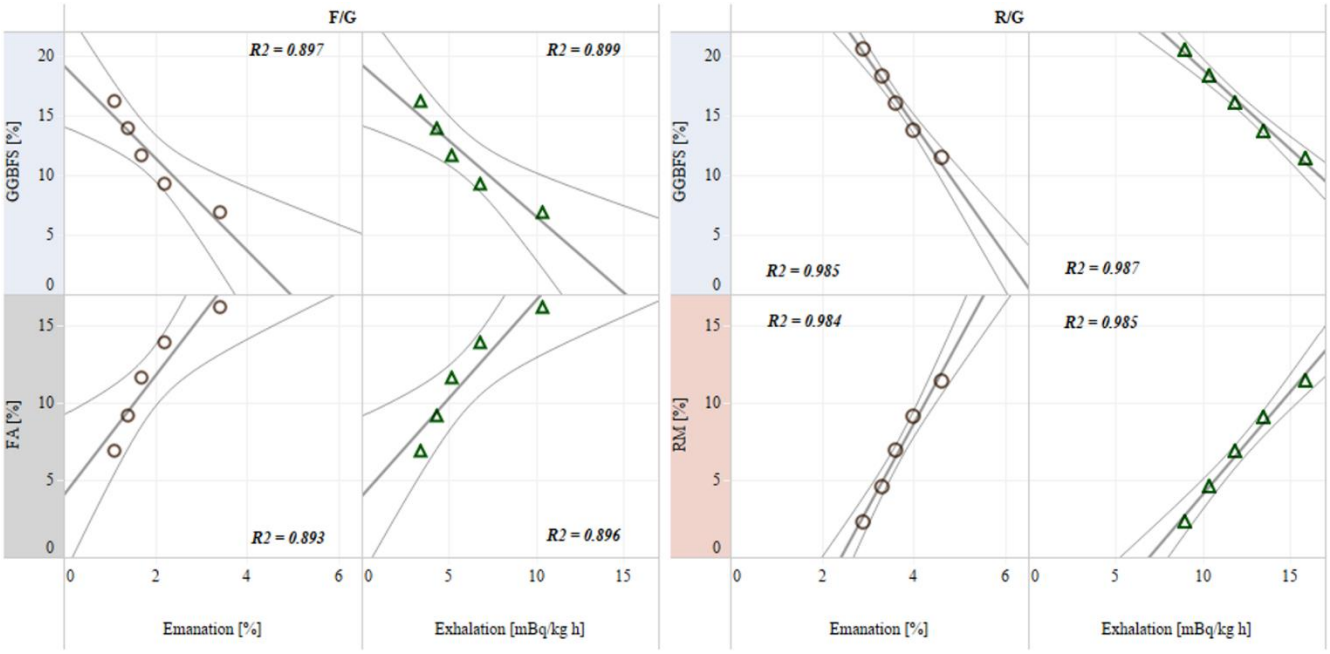

330

331 **Fig. 3**. The measured emanation and exhalation properties compared with the fly ash (FA), red mud (RM) and
332 ground granulated blast furnace slag (GGBFS) content in the fly ash and ground granulated blast furnace slag
333 (F/G) and red mud and ground granulated blast furnace slag (R/G) series where the trendlines were placed with
334 95% confidence bands.

335 In the case of the G series, the non-systematic sample composition did not make correlation analysis possible. In
336 the case of the F/G and R/G series, a strong correlation was found between the different component contents and
337 the emanation and exhalation properties. In both series, the increasing GGBFS content resulted in significantly
338 decreasing emanation (R^2 = 0.897 and 0.985) and exhalation (R^2 = 0.899 and 0.987), while the fly ash (emanation
339 R^2 = 0.893) (exhalation R^2 = 0.896) and the red mud (emanation R^2 = 0.984) (exhalation R^2 = 0.985) content
340 significantly increased both parameters.

341 In general, the mechanical properties are the primary objective of construction materials related research studies.
342 However, the radiological parameters are also critical to create safe building materials. The GGBFS, FA and the
343 GGBFS, red mud content, the I-index and the exhalation property of the final products were also compared with
344 the 28 days compressive strength (Fig. 4).

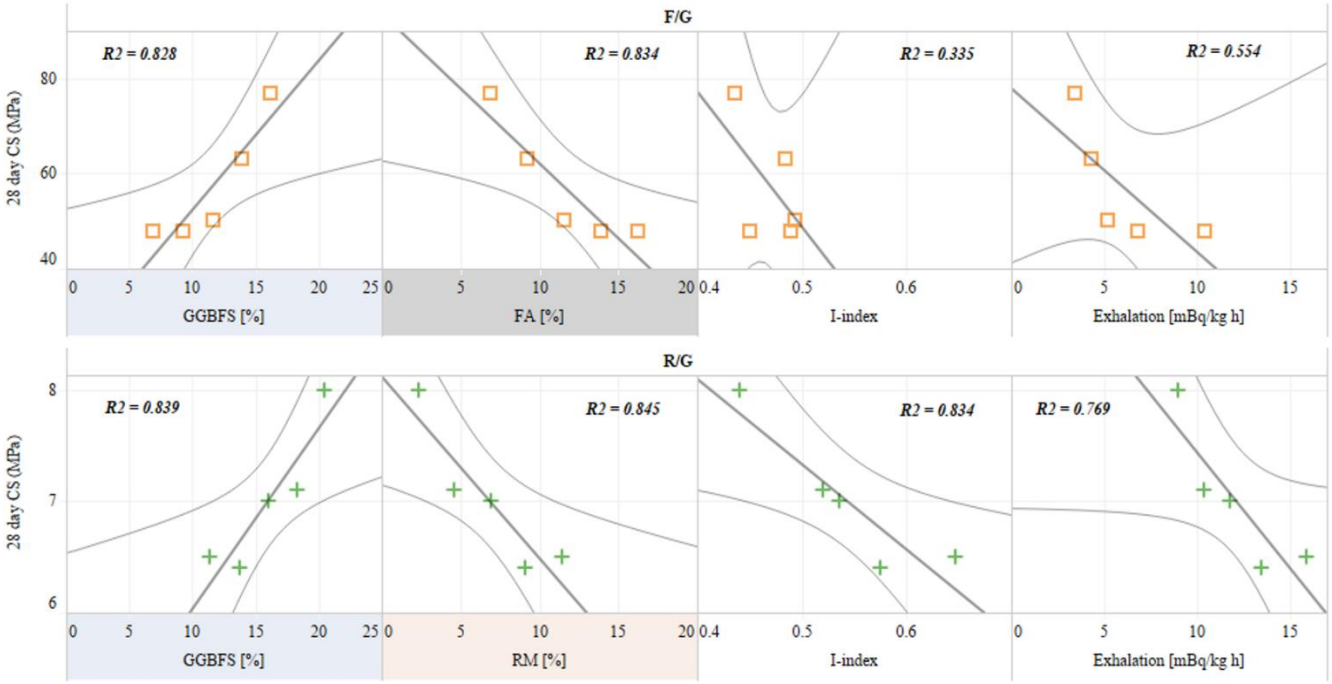

345

346 **Fig. 4**. Comparison of the fly ash (FA), red mud (RM) and ground granulated blast furnace slag (GGBFS) content,
347 I-index and exhalation with 28-day compressive strength (CS) properties in the fly ash and ground granulated blast
348 furnace slag (F/G) and red mud and ground granulated blast furnace slag (R/G) series where the trendlines were
349 placed with 95% confidence bands.

350 In the case of the G series, no correlation was found between the strength property and the GGBFS content within
351 the current test matrix. In the case of the F/G and the R/G series, the increasing GGBFS content resulted in
352 increased compressive strength, while the other secondary raw materials decreased the strength. The I-index of
353 the F/G and the R/G series showed a decreasing tendency with the compressive strength. Primarily, the R/G series
354 showed a strong negative correlation with the strength property. In the case of the F/G series, the NOR content of
355 the GGBFS and the FA was similar, so the final I-indexes of the mixes also were similar. In Fig. 3, the increasing
356 FA or red mud content correlated with a significantly increasing radon exhalation tendency, which was similar to
357 the case of the strength data. Those components also decreased the strength.

358

4. Conclusions

Three series of AAM mixes prepared from secondary raw materials (red mud, fly ash and ground granulated blast furnace slag) were investigated for their radiological properties including NOR content, I-index, radon emanation and exhalation. The NOR content of the secondary raw materials, when compared with international databases, was found to be lower than average, and the subsequent I-indexes of the AAM products were all below 1, which would initially suggest that they were acceptable for use in building products. The radon emanation and exhalation of the secondary raw materials and the subsequent AAM mixes were also determined. The emanation and the exhalation properties were also calculated for the AAM mixes, weighing the data of the secondary raw materials as a function of their mixing ratio in the AAM. The measured and the calculated results were compared and showed that the increasing fly ash content significantly enhanced the radon exhalation. This highlights that the formation of AAM cement matrix also plays an important role in the fate of radon transport from AAM building products, something that NOR content and I-indexes do not account for. Correlation analysis demonstrated that the increasing fly ash and red mud content significantly increased both emanation and exhalation parameters for both the F/G and R/G AAM mixes, whereas the GGBFS content lowered both emanation and exhalation parameters. The 28 days compressive strength was also compared with the secondary raw material content, and it was found that the higher GGBFS content resulted in higher strength. The GGBFS rich AAMs showed an inverse relationship with strength and radon exhalation, which can be attributed to the binding role of the GGBFS in the AAM matrixes. It can be stated that the most favourable strength and radiological properties were obtained when the GGBFS content was the highest compared to the amount of other secondary raw materials. Good design in relation to radon emanation and exhalation characteristics of construction materials made from secondary raw materials with elevated NOR content is essential especially as properties such as porosity, durability (microcracking), drying and shrinkage are inherently related to radon release and should be studied in parallel. This highlights the need to carry out exhalation testing on the final products as well as individual secondary raw materials.

Acknowledgements

The project leading to this paper has received funding from the European Union's Horizon 2020 research and innovation programme under the Marie Sklodowska-Curie grant agreement No 701932. R. Doherty's time was also supported by the European Union's Horizon 2020 research and innovation programme under the Marie Sklodowska-Curie grant agreement No 643087.

References

Aiken, T.A., Kwasny, J., Sha, W., Soutsos, M.N., 2018. Effect of slag content and activator dosage on the resistance of fly ash geopolymer binders to sulfuric acid attack. Cem. Concr. Res. 111, 23–40. https://doi.org/10.1016/j.cemconres.2018.06.011

Ayres, R.U., Holmberg, J., Andersson, B., 2001. Materials and the global environment: waste mining in the 21st century. MRS Bull. 26, 477–480. https://doi.org/10.1557/mrs2001.119

Bondar, D., Thompson, D., Nanukuttan, S., Soutsos, M., Basheer, M., 2016. Resistance of alkali activated slag concretes to chloride environments, in: Proceedings of Civil Engineering Research in Ireland Conference, Nanukuttan S. and Goggins J. (Eds), National University of Ireland Galway. Civil Engineering Research Association of Ireland, pp. 265–270.

Bontempi, E., 2017. A new approach for evaluating the sustainability of raw materials substitution based on embodied energy and the CO_2 footprint. J. Clean. Prod. 162, 162–169. https://doi.org/10.1016/j.jclepro.2017.06.028

BS EN 12390-3, 2009. Testing hardened concrete–Part 3: compressive strength of test specimens. British Standards Institution (BSI).

BS EN 15167-1, 2006. Ground granulated blast furnace slag for use in concrete, mortar and grout–Part 1: definitions, specifications and conformity criteria. British Standards Institution (BSI).

BS EN 450-1, 2012. Fly ash for concrete–Part 1: definition, specifications and conformity criteria. British Standards Institution (BSI).

Darby, S., Hill, D., Auvinen, A., Barros-Dios, J.M., Baysson, H., Bochicchio, F., Deo, H., Falk, R., Forastiere, F., Hakama, M., Heid, I., Kreienbrock, L., Kreuzer, M., Lagarde, F., Mäkeläinen, I., Muirhead, C., Oberaigner, W., Pershagen, G., Ruano-Ravina, A., Ruosteenoja, E., Rosario, A.S., Tirmarche, M., Tomáscaron;ek, L., Whitley, E., Wichmann, H.-E., Doll, R., 2005. Radon in homes and risk of lung cancer: collaborative analysis of individual data from 13 European case-control studies. BMJ 330, 223. https://doi.org/10.1136/bmj.38308.477650.63

Dubois, G., Bossew, P., 2006. A European Atlas of Natural Radiations including harmonized radon maps of the European Union. What do we have, what do we know, quo vadimus?, in: ARPA Piemonte - Atti Del Terzo Convegno Nazionale Sugli Agenti Fisici. pp. 1–6.

EEA-JRC, 2013. Environment and human health: joint EEA-JRC report. Publications Office of the European Union.

European Commission, 2015. An EU action plan for the circular economy. Com 614, 21.

European Union, 2014. Council Directive 2013/59/Euratom of 5 December 2013 laying down basic safety standards for protection against the dangers arising from exposure to ionising radiation, and repealing Directives 89/618/Euratom, 90/641/Euratom, 96/29/Euratom, 97/43/Euratom a. Off. J. Eur. Commun. L13, 1–73. https://doi.org/10.3000/19770677.L_2014.013.eng

Friedmann, H., Nuccetelli, C., Michalik, B., Anagnostakis, M., Xhixha, G., Kovler, K., de With, G., Gascó, C., Schroeyers, W., Trevisi, R., Antropov, S., Tsapalov, A., Kunze, C., Petropoulos, N.P., 2017. Measurement of NORM, in: Naturally Occurring Radioactive Materials in Construction. Elsevier, pp. 61–133. https://doi.org/10.1016/B978-0-08-102009-8.00005-0

Gijbels, K., Iacobescu, R.I., Pontikes, Y., Vandevenne, N., Schreurs, S., Schroeyers, W., 2018. Radon immobilization potential of alkali-activated materials containing ground granulated blast furnace slag and

phosphogypsum. Constr. Build. Mater. 184, 68–75. https://doi.org/10.1016/j.conbuildmat.2018.06.162

Härdle, W., Werwatz, A., Müller, M., Sperlich, S., 2004. Nonparametric Density Estimation. Springer, pp. 39–83. https://doi.org/10.1007/978-3-642-17146-8_3

Hegedus, M., Sas, Z., Toth-Bodrogi, E., Szanto, T., Somlai, J., Kovacs, T., 2016. Radiological characterization of clay mixed red mud in particular as regards its leaching features. J. Environ. Radioact. 162–163, 1–7. https://doi.org/10.1016/j.jenvrad.2016.05.002

Jonas, J., Sas, Z., Vaupotic, J., Kocsis, E., Somlai, J., Kovacs, T., 2016. Thoron emanation and exhalation of Slovenian soils determined by a PIC detector-equipped radon monitor. Nukleonika 61, 379–384. https://doi.org/10.1515/nuka-2016-0063

Keller, G., Hoffmann, B., Feigenspan, T., 2001. Radon permeability and radon exhalation of building materials. Sci. Total Environ. 272, 85–89. https://doi.org/10.1016/S0048-9697(01)00669-6

Kovacs, T., Bator, G., Schroeyers, W., Labrincha, J., Puertas, F., Hegedus, M., Nicolaides, D., Sanjuán, M.A., Krivenko, P., Grubeša, I.N., Sas, Z., Michalik, B., Anagnostakis, M., Barisic, I., Nuccetelli, C., Trevisi, R., Croymans, T., Schreurs, S., Todorović, N., Vaiciukyniene, D., Bistrickaite, R., Tkaczyk, A., Kovler, K., Wiegers, R., Doherty, R., 2017a. From raw materials to NORM by-products, in: Naturally Occurring Radioactive Materials in Construction. Elsevier, pp. 135–182. https://doi.org/10.1016/B978-0-08-102009-8.00006-2

Kovacs, T., Shahrokhi, A., Sas, Z., Vigh, T., Somlai, J., 2017b. Radon exhalation study of manganese clay residue and usability in brick production, J. Environ. Radioact. 168, 15–20. https://doi.org/10.1016/j.jenvrad.2016.07.014

Rafeet, A., 2016. Mix design, fresh and hardened properties and microstructural characterisation of alkali-activated concrete based on PFA/GGBS blends, PhD thesis. Queen's University Belfast ISNI: 0000 0004 6059 5421.

Sahoo, B.K., Sapra, B.K., Gaware, J.J., Kanse, S.D., Mayya, Y.S., 2011. A model to predict radon exhalation from

walls to indoor air based on the exhalation from building material samples. Sci. Total Environ. 409, 2635–2641. https://doi.org/10.1016/j.scitotenv.2011.03.031

Sainz, C., Dinu, A., Dicu, T., Szacsvai, K., Cosma, C., Quindós, L.S., 2009. Comparative risk assessment of residential radon exposures in two radon-prone areas, Ştei (Romania) and Torrelodones (Spain). Sci. Total Environ. 407, 4452–4460. https://doi.org/10.1016/j.scitotenv.2009.04.033

Sas, Z., Somlai, J., Jonas, J., Szeiler, G., Kovacs, T., Gyongyosi, C., Sydo, T., 2013. Radiological survey of Hungarian clays; radon emanation and exhalation influential effect of sample and internal structure conditions. Rom. Reports Phys. 58, 243–250.

Sas, Z., Szanto, J., Kovacs, J., Somlai, J., Kovacs, T., 2015a. Influencing effect of heat-treatment on radon emanation and exhalation characteristic of red mud. J. Environ. Radioact. 148, 27–32. https://doi.org/10.1016/j.jenvrad.2015.06.002

Sas, Z., Hegedus, M., Szanto, J., Somlai, J., Kovacs, T., 2015b. Radon/thoron exhalation characteristic of heat treated red mud, relationship between internal structure features, possibilities of reduction, Bauxite Residue Valorization and Best Practices Conference, Leuven, Belgium.

Sas, Z., Doherty, R., Kovacs, T., Soutsos, M., Sha, W., Schroeyers, W., 2017. Radiological evaluation of by-products used in construction and alternative applications; Part I. Preparation of a natural radioactivity database. Constr. Build. Mater. 150, 227–237. https://doi.org/10.1016/j.conbuildmat.2017.05.167

Sas, Z., Vandevenne, N., Doherty, R., Vinai, R., Kwasny, J., Russell, M., Sha, W., Soutsos, M., Schroeyers, W., 2019. Radiological evaluation of industrial residues for construction purposes correlated with their chemical properties. Sci. Total Environ. 658, 141–151. https://doi.org/10.1016/j.scitotenv.2018.12.043

Schroeyers, W., Sas, Z., Bator, G., Trevisi, R., Nuccetelli, C., Leonardi, F., Schreurs, S., Kovacs, T., 2018. The NORM4Building database, a tool for radiological assessment when using by-products in building materials. Constr. Build. Mater. 159, 755–767. https://doi.org/10.1016/j.conbuildmat.2017.11.037

476 Shakhashiro, A., Tarjan, S., Ceccatelli, A., Kis-Benedek, G., Betti, M., 2012. IAEA-447: A new certified reference
477 material for environmental radioactivity measurements. Appl. Radiat. Isot. 70, 1632–1643.
478 https://doi.org/10.1016/j.apradiso.2012.03.024

479 Trevisi, R., Leonardi, F., Risica, S., Nuccetelli, C., 2018. Updated database on natural radioactivity in building
480 materials in Europe. J. Environ. Radioact. 187, 90–105.
481 https://doi.org/https://doi.org/10.1016/j.jenvrad.2018.01.024

482 United Nations Scientific Committee on the Effects of Atomic Radiation, 2010. Annex B: Exposures of the public
483 and workers from various sources of radiation, UNSCEAR 2008 Report to the general assembly with
484 scientific annexes. United Nations, New York.

485 Van Deventer, J.S.J., Provis, J.L., Duxson, P., Brice, D.G., 2010. Chemical research and climate change as drivers
486 in the commercial adoption of alkali activated materials. Waste Biomass Valori. 1, 145–155.
487 https://doi.org/10.1007/s12649-010-9015-9

488 Vasilyev, A., Yarmoshenko, I., Zhukovsky, M., 2017. Radon safety in terms of energy efficiency classification of
489 buildings. IOP Conf. Ser. Earth Environ. Sci. 72, 012020. https://doi.org/10.1088/1755-1315/72/1/012020

490 WHO, 2016. Radon and health fact sheet [WWW Document]. World Heal. Organ. URL
491 http://www.who.int/mediacentre/factsheets/fs291/en/ (accessed 4.5.18).